ARTICLES

Postcranial evidence from early *Homo* from Dmanisi, Georgia

David Lordkipanidze[1], Tea Jashashvili[1,2], Abesalom Vekua[1], Marcia S. Ponce de León[2], Christoph P. E. Zollikofer[2], G. Philip Rightmire[3], Herman Pontzer[4], Reid Ferring[5], Oriol Oms[6], Martha Tappen[7], Maia Bukhsianidze[1], Jordi Agusti[8], Ralf Kahlke[9], Gocha Kiladze[1], Bienvenido Martinez-Navarro[8], Alexander Mouskhelishvili[1], Medea Nioradze[10] & Lorenzo Rook[11]

The Plio-Pleistocene site of Dmanisi, Georgia, has yielded a rich fossil and archaeological record documenting an early presence of the genus *Homo* outside Africa. Although the craniomandibular morphology of early *Homo* is well known as a result of finds from Dmanisi and African localities, data about its postcranial morphology are still relatively scarce. Here we describe newly excavated postcranial material from Dmanisi comprising a partial skeleton of an adolescent individual, associated with skull D2700/D2735, and the remains from three adult individuals. This material shows that the postcranial anatomy of the Dmanisi hominins has a surprising mosaic of primitive and derived features. The primitive features include a small body size, a low encephalization quotient and absence of humeral torsion; the derived features include modern-human-like body proportions and lower limb morphology indicative of the capability for long-distance travel. Thus, the earliest known hominins to have lived outside of Africa in the temperate zones of Eurasia did not yet display the full set of derived skeletal features.

Since 1991 hominin remains have been recovered from excavation blocks 1 and 2 at Dmanisi, Georgia. Three skulls (D2282/D211, D2700/D2735 and D3444/D3900), one cranium (D2280) and one mandible (D2600) have been described earlier[1–7]. The well-preserved postcranial remains recovered from block 2 provide an insight into previously unknown aspects of early *Homo* morphology and also offer a new comparative perspective on key elements of the postcranial skeleton of the Nariokotome KNM-WT15000 subadult specimen[8] and of *Homo floresiensis*[9].

Stratigraphical context

The geological age of the bone- and artefact-bearing deposits at Dmanisi is approximately 1.77 million years (Myr)[10]. New palaeomagnetic analyses of block 2 deposits are fully concordant with the initial stratigraphical and palaeomagnetic studies of block 1 (Supplementary Information 1). Consideration of the overall mammalian fauna places the site close to the Plio-Pleistocene boundary and shows highest palaeozoogeographical similarity with the chronologically contemporaneous Late Villafranchian of Western Europe (Supplementary Information 2 and 3). Palaeoecological studies point to a remarkable variation in relief, humidity and vegetational character. The presence of fresh water and a variety of ecotones with different vegetal and animal resources nearby made Dmanisi an attractive locale for hominins (Supplementary Information 2–4). Analysis of the taphonomic signature of mammalian remains indicates that hominins were involved in meat acquisition, and that they had early access to carcasses, which suggests hunting or power scavenging. Carnivores were also active at the site, but did not damage bone to the degree found in many hyaena dens (Supplementary Information 5).

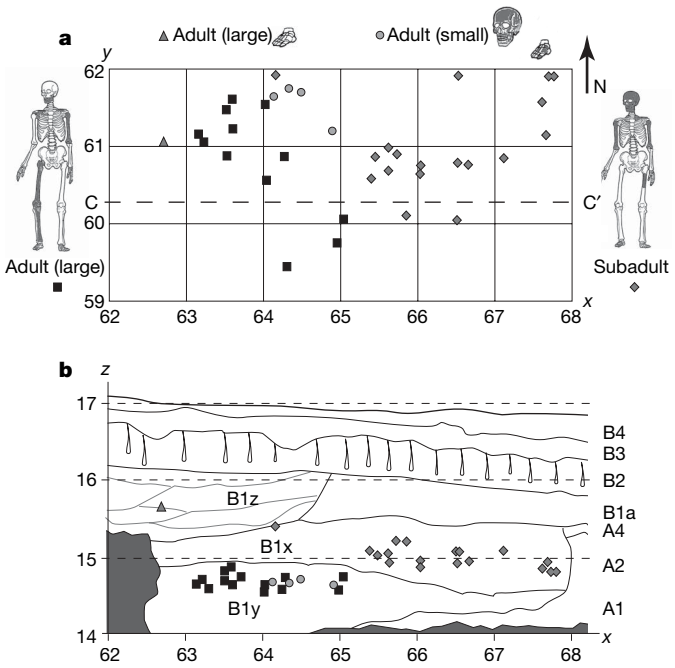

Figure 1 | Stratigraphy of the Dmanisi postcranial hominin remains recovered from block 2. a, Vertical projection (*x*–*y* excavation squares are 1 × 1 m; *in-situ* articulated cervical vertebrae D2673/D2674 are denoted by the double diamond). **b**, Lateral projection along *y* axis (profile section taken along C–C′) and *z* axis (metres above zero level reference, see also Supplementary Fig. 1).

[1]Georgian National Museum, 0105 Tbilisi, Georgia. [2]Anthropologisches Institut, Universität Zürich, 8057 Zürich, Switzerland. [3]Department of Anthropology, Peabody Museum, Harvard University, Cambridge, Massachusetts 02138, USA. [4]Department of Anthropology, Washington University, St Louis, Missouri 63130, USA. [5]Department of Geography, University of North Texas, Denton, Texas 76203, USA. [6]Departament de Geologia, Universitat Autònoma de Barcelona, 08193 Bellaterra, Spain. [7]Department of Anthropology, University of Minnesota, Minneapolis, Minnesota 55455, USA. [8]ICREA, Institute of Human Paleoecology, University Rovira i Virgili, 43005 Tarragona, Spain. [9]Senckenberg Research Institute, 99423 Weimar, Germany. [10]Othar Lordkipanidze Center for Archaeological Research, 0102 Tbilisi, Georgia. [11]Dipartimento di Scienze della Terra, Università di Firenze, 50121 Firenze, Italy.

The new hominin skeletal elements from Dmanisi can be assigned to a minimum of four individuals: one adolescent and three adults (Figs 1 and 2). The postcranial remains of the adolescent individual are associated with skull D2700/D2735 (ref. 3). Attribution of all adolescent remains to one individual is based on their close stratigraphical proximity within layer B1x (Fig. 1) and equivalent developmental stages of cranial and postcranial elements (Supplementary Table 3). The spatial distribution pattern of these elements, their uniform stage 0/1 taphonomic condition[11], as well as the partial laminated infilling of the D2700 and D3444 cranial vaults[7], indicate short-distance, low-energy dispersal followed by rapid burial (Supplementary Information 1).

Postcranial remains of three adult individuals, found in layer B1y, exhibit virtually no stratigraphical overlap with the adolescent remains (Fig. 1). These elements are provisionally attributed to one large and two small individuals. The large adult is represented by various elements of the appendicular skeleton. The right femur, tibia and patella exhibit fit in the knee joint, and the left talus, when mirrored to the right side, implies anatomical fit with the tibia. These postcranial remains are probably associated with the large mandible D2600 (ref. 4) found nearby in the same stratigraphical layer (Fig. 1 and Supplementary Fig. 1). Postcranial elements of one smaller adult individual comprise a right medial cuneiform and anatomically associated metatarsal I, and are presumably associated with the small skull D3444/D3900 (refs 5, 7) found nearby. A third adult individual is currently represented by a single metatarsal II found at a higher stratigraphical position (layer B1z; see Fig. 1). Measurements are provided in Table 1, Fig. 3 and Supplementary Information 7.

Upper limbs

D4166 is the lateral part of an adult right scapula comprising the glenoid cavity, and exhibiting some damage across the distal part of the coracoid process. The glenoid cavity is more cranially oriented relative to the midaxillary border than in modern humans, and thus closer to the condition found in australopiths (Sts7 and AL288-1)[12,13] and African great apes. The narrow glenocoracoid angle, the relatively short coracoid process, and the high width-to-length ratio of the coracoid process are outside the range of variation found in modern humans, and are similar to great apes[14], whereas the glenoid orientation relative to the spine and the breadth-to-width ratio of the spine are at the lower end of modern-human variation and similar to KNM-WT15000. D4161 and D4162 are left and right adult

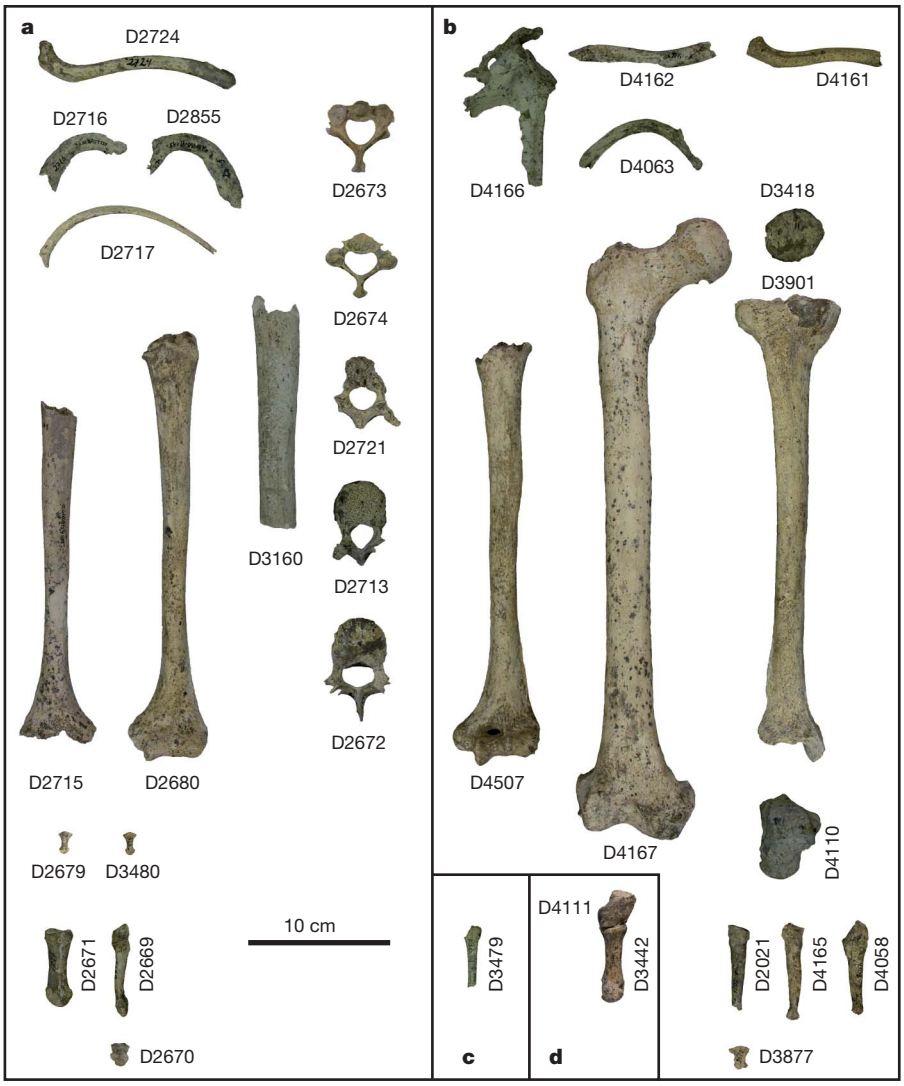

Figure 2 | Dmanisi postcranial elements. a, Remains of subadult individual. D2724, left clavicle; D2716/D2855, right/left first rib; D2717, eleventh rib; D2673/D2674/D2721/D2713/D2672, vertebrae C2/C3/Th3/Th10/L1; D2715/D2680, right/left humerus; D3160, left femur; D2679/D3480, distal phalanges of hand; D2671/D2669, right metatarsal I/IV; D2670, first distal phalange of right foot. **b**, Remains of large adult individual. D4166, right scapula; D4162/D4161, right/left clavicles; D4063, right second rib; D4507, left humerus; D4167, right femur; D3418, right patella; D3901, right tibia; D4110, left talus; D2021/D4165, right metatarsals III/IV; D4508, left metatarsal V; D3877, distal phalange of foot. **c**, **d**, Remains of small adult individuals. D3479, right metatarsal III; D4111, right medial cuneiform; D3442, right metatarsal I.

clavicles, respectively. Both elements lack their sternal and acromial ends. D2724 is an almost complete subadult left clavicle with some damage at the epiphyses. The shaft is comparatively short, similar to Chk-B-2-81 (Zhoukoudian *Homo erectus*)[15] and OH48 (*Homo habilis*)[16], but within the range of variation displayed by subadult modern humans. In their mid-shaft and conoid tubercular cross-sectional shape, all Dmanisi clavicles are more similar to modern humans and Chk-B-2-81/OH48 than to KNM-WT15000, which has a greater antero-posterior than supero-inferior diameter. D2680 and D2715 are left and right subadult humeri; D4507 is a left adult humerus. In both individuals, the humeral shaft is almost straight, and the position of the lateral epicondyle in relation to the lateral condyle is comparatively high. This is different compared with the condition found in modern humans, but similar to Plio-Pleistocene hominins[17] and African great apes. Humeral torsion in the Dmanisi sample is virtually absent, similar to australopiths (AL288-1, Sts7, KNM-ER739)[18] and *H. floresiensis*[19] (LB1), whereas the KNM-WT15000 humeri are at the lower end of variation of modern-human-like degrees of torsion.

Axial skeleton

The vertebral column of the subadult individual is represented by five elements: D2673 (cervical 2 (C2), axis), D2674 (C3), D2721 (thoracic ~3 (Th3)), D2713 (thoracic ~10 (Th10)) and D2672 (lumbar 1 (L1)). In C2, the superior articular process is sloping downwards mediolaterally, as in the great apes and australopiths, but the spinal process is short and narrow, similar to the condition found in modern humans and australopiths. Canal shapes of all vertebrae are wider transversally than dorso-ventrally, similar to AL333-101, KNM-WT15000 and modern humans. Zygapophyseal joint orientation of C3, Th10 and L1 is like that in modern humans. The centra of Th10 and L1 are transversally extended; T10 exhibits anterior wedging, whereas L1 exhibits slight posterior wedging.

Lower limbs

The adult right femur, tibia and patella constitute the most complete lower limb of early *Homo* recovered so far. D4167 is a complete right femur with a well-developed linea aspera. The shaft is markedly more robust than that of KNM-ER1481a[20] (early *Homo*). The neck index is similar to australopiths and KNM-WT15000, but lower than in modern humans. As in all hominins[21], the greater trochanter is less elevated than the head but is laterally prominent. In keeping with the low degree of anteversion (femoral torsion), the lesser trochanter is not carried far towards the medial margin of the shaft[22]. Like Asian and African *H. erectus*, the Dmanisi femur has a narrow medullary canal[21] in comparison to modern humans. The shaft is straight in anterior view and displays the valgus orientation characteristic for hominins. The distal bicondylar angle is within the range of variation of australopiths and early *Homo*[23], and at the upper extreme of modern human variation. D3418 is a right patella. The medial surface is larger than the lateral surface, which is unusual in modern humans. The mediolateral breadth is slightly larger than that of the left patella SKX 1084 (ref. 24) from Swartkrans Member 2. D3901 is the first complete fossil hominin tibia. It is comparatively robust; the proximal and distal joint surfaces and the malleolus are large relative to diaphyseal length (Fig. 3a), but mid-shaft proportions are like those of early *Homo* (KNM-ER803b, KNM-ER741)[25,26]. D3901 is similar to modern human tibiae in its degree of torsion, but clearly different in its degree of inclination. This latter feature is pronounced in humans, but not in great apes.

Table 1 | Postcranial dimensions of the Dmanisi hominins

Measurements	Australopiths	Earliest *Homo*	Dmanisi	KNM-WT15000	Modern humans
Shoulder girdle					
Olecranon orientation relative to midaxillary border (M17) (°)	115.0–116.0†	–	129.0	*127.0*	133.8–154.0
Glenocoracoid angle (°)	–	–	55.0	*59.5*	60.0–94.5
Clavicular length (M1) (mm)	–	149.4‡	137.3 (L), 135.6 (R), *123.2*	*130.5*	113.0–159.0, *113.0–139.0*
Humerus					
Length (M1) (mm)	226.0–235.0§	–	295.0, *282.2*	*319.0*	263.0–341.0, *255.0–334.0*
Mid-shaft a–p diameter (mm)	19.0	–	37.1, *17.1 (L), 16.8 (R)*	*19.9*	16.5–36.0, *12.5–24.3*
Mid-shaft m–l diameter (mm)	15.0	–	34.8, *14.3 (L), 14.7 (R)*	*16.7*	11.5–24.5, *13.3–31.4*
Torsion (M18) (°)	111.0–130.0‖	–	110.0, *104.0*	*126.0*	134.9–180.0, *138.2–160.7*
Vertebrae					
C2 anterior angle of superior articular process (°)	107.0–120.0¶	–	*111.0*	–	*129.1–147.2*
C2/C3 zygapophyseal joint angle (°)	–	–	*62.5*	–	*62.0–85.0*
Th10 centrum area (M4*M7) (mm^2)	–	–	*692.2*	–	*601.1–958.6*
L1 centrum area (M4*M7) (mm^2)	–	–	*777.8*	*803.4*	*706.3–1,288.9*
Femur					
Length (M1) (mm)	280.0#	401.0–396.0☆	386.0	*432.0*	337.0–434.0
Head diameter (M19) (mm)	27.9–39.4**	40.0–42.0☆	40.0	*46.0*	42.7–55.1
Mid-shaft a–p diameter (M6) (mm)	22.0#	27.7–28.8☆	26.5	*24.5*	29.1–34.7
Mid-shaft m–l diameter (M7) (mm)	21.0#	26.4–25.6☆	22.2	*24.3*	26.1–29.9
Medial condylar breadth (M21c) (mm)	19.3–22.3††	20.7–21☆	24.2	–	27.6–40.3
Lateral condylar breadth (M21e) (mm)	17.9–22.1††	19.2–25.5☆	23.3	–	24.2–32.9
Bicondylar angle (M30) (°)	75.0–81.0‡‡	77.0–80.0☆	81.5	*80.0*	76.0–88.0
Tibia					
Length (M1a) (mm)	–	–	306.0	*380*	290.0–374.0
Mid-shaft a–p diameter (M8) (mm)	–	22.5–31.0§§	27.0	*24.5*	25.8–42.3
Mid-shaft m–l diameter (M9) (mm)	–	14.6–23.6§§	18.0	*20.4*	15.5–24.6
Angle of inclination (M13) (°)	–	–	82.0	–	89.1–111.7
Foot					
Neck angle of talus (M16) (°)	32.3‖‖	33.5¶¶	26.0	–	12.0–31.0
Estimates*					
Stature (cm)	110.0–151.0 (ref. 50)	125.0–157.0 (ref. 50)	144.9–166.2	*150.5–169.1* (ref. 42)	–
Body mass (kg)	29.0–49.0 (ref. 50)	32.0–52.0 (ref. 50)	40.0–50.0	*45.5–70.6* (ref. 42)	–
Encephalization quotient	2.4–3.1 (ref. 50)	3.1 (ref. 50)	2.57–3.13	*2.71–3.78*	6.3

Measurement ranges were used for australopiths and modern humans. Data for subadults are in italic font. a–p, antero-posterior; m–l, mediolateral. For measurement codes (M1, M7, and so on) see ref. 69 of Supplementary Information.

* See Supplementary Table 6 for details on estimation procedures. †Sts7, AL288-1. ‡OH48. §AL288-1, Bou-VP-12/1. ‖AL288-1, ER739, Sts7, Omo119. ¶AL333-101, SK-854. #AL288-1. ☆KNM-ER1481, KNM-ER1472. **AL288-1, AL333-4. ††AL129, AL333-4, Sts34, TM1513. ‡‡AL288-1, AL129-1a, AL333-4, AL333w-56, Sts34, TM1513, ER993. §§OH35a, ER813a, ER741. ‖‖AL288-1, TM1517, ER1476a, ER813, ER1464, Stw573. ¶¶OH8.

Foot bones

D4110 is a well-preserved left talus. The neck is stout and expanded transversely but elongated compared to modern humans. The neck (horizontal) angle is small and similar to modern humans[27]. The medial tubercle is strong and projecting, and the groove for the tendon of flexor hallucis longus is deep. This groove has a slightly oblique orientation, which is similar to great apes, whereas humans exhibit a more vertical orientation[28]. D2671 and D3442 are subadult and adult right first metatarsals, respectively, with lengths at the lower end of modern human variation and elevated robusticity indices. The morphology of the head deviates from that known from apes and humans. It is spherical and exhibits a narrowing of the dorsal breadth of the articular surface[29]. Head torsion is in the range of variation of subadult and adult modern humans and of OH8 (*H. habilis*)[30]. Two adult metatarsals III (D2021 and D3479) have a straight shaft, exhibit a high degree of torsion and have a dorso-ventrally elongated cross-sectional shape, as in modern humans. Metatarsals IV (adult D4165 and subadult D2669) exhibit an elevated degree of torsion and dorso-ventral elongation. Adult metatarsal V (D4508) is short and at the lower end of modern human variation for its mid-shaft dimensions.

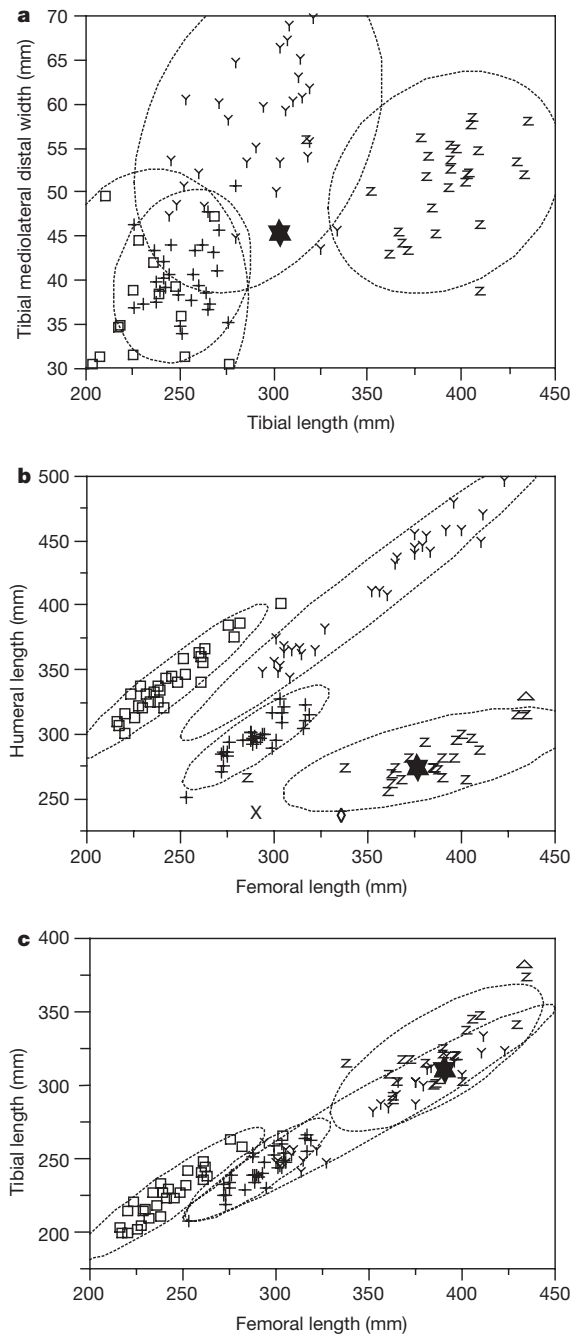

Figure 3 | Long-bone shape and proportions. **a**, Tibial mediolateral distal width versus maximum length. **b**, Humeral versus femoral length. **c**, Tibial versus femoral length. Stars, Dmanisi *Homo*; X, AL288-1 (*Australopithecus afarensis*); diamond, BOU-VP-12/1; triangle, KNM-WT15000 (*H. erectus*); Z, recent *Homo sapiens*; plus signs, *Pan troglodytes*; Y, *Gorilla gorilla*; squares, *Pongo pygmaeus*.

Evolutionary and functional context

The postcranial morphology of the australopiths is best documented by the AL288-1 specimen[31], indicating that their stature was small (105 cm) and their limb proportions between those of great apes and modern humans, suggesting terrestrial bipedalism with retained arboreal locomotor capabilities. Contrastingly, the postcranial morphology of earliest *Homo* (cf. *H. habilis*) is known from only a few fragmentary specimens (for example, OH35, OH62, KNM-ER3735 (refs 32–35)) dated between 1.75- and 1.9-Myr ago[36,37], such that inferences regarding the evolution of stature and limb proportions in this genus are a matter of ongoing debate[38–40]. The first well-documented evidence for the postcranium of genus *Homo* comes from the KNM-WT15000 specimen, dated to approximately 1.55 Myr ago, the body proportions and stature of which are modern in almost every aspect[8]. Information about the transition from australopith-like to modern-human-like postcranial morphologies is thus rather limited, and the Dmanisi postcranial material fills significant gaps in our knowledge about this critical period of hominin evolution.

The presence of anatomically matching proximal and distal lower limb bones (D4167 and D3901) in the Dmanisi sample and the likely association of these elements with humerus D4507 can be used to infer stature and limb proportions. Stature and body mass of the Dmanisi individuals calculated from various independent long bone measurements yield estimates between 145–166 cm and 40–50 kg, respectively (Table 1 and Supplementary Information 8). Their small stature might be interpreted in two different, but non-exclusive, ways. On the one hand, it might represent a plesiomorphic character shared with earliest *Homo* (cf. *H. habilis*) (125–157 cm and 32–52 kg[41]), whereas the KNM-WT15000 specimen appears to be derived in this respect (150.5–169.1 cm and 45.5–70.6 kg)[42]. On the other hand, differences in stature between the Dmanisi and KNM-WT15000 hominins might reflect adaptation to different palaeo-ecological contexts. Limb proportions of the Dmanisi hominins, measured by femoral/tibial and humeral/femoral ratios (Fig. 3b, c and Table 1), were similar to those of modern humans, but also to those of earliest African *Homo* and to the BOU-VP-12/1 specimen dated to 2.5 Myr ago[43]. Absolute hindlimb length of the Dmanisi hominins is greater than in australopiths and close to that of later *Homo* including modern humans. This may reflect selection for improved locomotor energy efficiency, as the cost of transport is inversely proportional to hindlimb length for terrestrial animals including bipeds[44].

Cranial capacities (roughly equivalent to brain volume) for the Dmanisi individuals vary from 600 to 775 cm^3 (refs 2, 3, 7). These values overlap with *H. habilis* (614 ± 66 cm^3; $n = 6$)[45], but are more than one standard deviation below the mean for *H. erectus* (904 ± 100 cm^3; $n = 13$)[46]. Combining cranial and postcranial dimensions, the encephalization quotient for the Dmanisi individuals is in the range of 2.6 to 3.1 (Table 1 and Supplementary Table 6), which is at the lower end of estimates for KNM-WT15000 (2.7–3.8) and more comparable to *H. habilis* (3.1) and australopiths (2.4–3.1).

Using modern human dental and postcranial developmental scores, the age difference between the Dmanisi and KNM-WT15000 specimens is around 2 yr (assuming individual ages of 11–13 and 8–10 yr, respectively), so these specimens are broadly comparable to each other. Overall vertebral morphology indicates

that the Dmanisi spine was more similar to that of early *H. erectus* and modern humans than to australopiths. Vertebral wedging is indicative of lumbar lordosis; zygapophyseal joint orientation suggests expanded ranges of spinal flexion; and the relatively large vertebral cross-sectional areas are indicative of resistance to increased compressive loads characteristic of running and long-range walking[47].

Humeral torsion is an important variable that influences orientation and ranges of movement of the upper limb relative to the trunk. In modern humans, the high degree of torsion is seen as a compensation for the more dorsal position of the scapula[18]. The low degree of torsion in the Dmanisi sample could thus indicate a habitually more abducted/supine orientation of the arm, a more lateral position of the shoulder girdle, and also a diverse range of arm movement. Reduced torsion in the throwing arm of athletes requiring high upper limb mobility (external rotation)[48] suggests developmental plasticity, but because this feature is not lateralized in the Dmanisi subadult individual, it might be interpreted as part of a plesiomorphic configuration of the upper body that also includes a more cranial orientation of the glenoid cavity of the scapula, a short coracoid process and a narrow glenocoracoid angle. Following this line of argument, the Dmanisi hominins would have had a more australopith-like than human-like upper limb morphology[49], and absence of humeral torsion in *H. floresiensis*[9] would provide support for the hypothesis of long-term continuity of this plesiomorphic trait in *Homo*.

Preservation in the Dmanisi remains of lower limb elements from the femur down to the metatarsals permits reconstruction of the positioning and orientation of the foot relative to the walking direction. The tibia exhibits slight medial torsion, and the talar neck angle is wide. This combination results in a more medial orientation of the foot, and a more equal load distribution on all rays than in modern humans. Although this configuration probably represents the plesiomorphic condition, various features of the Dmanisi foot are similar to modern humans and thus clearly derived: metatarsal torsion indicates the presence of a transverse arch; the wide base of the first metatarsal suggests a strong plantar ligament associated with a well-developed longitudinal arch[29]; and the flat proximal articular surface of the first metatarsal indicates that the hallux had an adducted position.

The following preliminary conclusions can be drawn: the morphology of the upper and lower limbs from Dmanisi exhibits a mosaic of traits reflecting both selection for improved terrestrial locomotor performance and the retention of primitive characters absent in later hominins (Supplementary Table 8). The length and morphology of the hindlimb is essentially modern, and the presence of an adducted hallux and plantar arch indicate that the salient aspects of performance in the leg and foot, such as biomechanical efficiency during long-range walking and energy storage/return during running, were equivalent to modern humans. However, plesiomorphic features such as a more medial orientation of the foot, absence of humeral torsion, small body size and low encephalization quotient suggest that the Dmanisi hominins are postcranially largely comparable to earliest *Homo* (cf. *H. habilis*). Hence, the first hominin species currently known from outside Africa did not possess the full suite of derived locomotor traits apparent in African *H. erectus* and later hominins.

Received 16 April; accepted 30 July 2007.

1. Gabunia, L. & Vekua, A. A. Plio-Pleistocene hominid from Dmanisi, East Georgia, Caucasus. *Nature* **373,** 509–512 (1995).
2. Gabunia, L. *et al.* Earliest Pleistocene hominid cranial remains from Dmanisi, Republic of Georgia: Taxonomy, geological setting, and age. *Science* **288,** 1019–1025 (2000).
3. Vekua, A. *et al.* A new skull of early *Homo* from Dmanisi, Georgia. *Science* **297,** 85–89 (2002).
4. Gabunia, L., de Lumley, M.-A., Vekua, A., Lordkipanidze, D. & de Lumley, H. Découverte d'un nouvel hominidé à Dmanissi (Transcaucasie, Géorgie). *C.R. Palévol.* **1,** 243–253 (2002).
5. Lordkipanidze, D. *et al.* The earliest toothless hominin skull. *Nature* **434,** 717–718 (2005).
6. Rightmire, G. P., Lordkipanidze, D. & Vekua, A. Anatomical descriptions, comparative studies and evolutionary significance of the hominin skulls from Dmanisi, Republic of Georgia. *J. Hum. Evol.* **50,** 115–141 (2006).
7. Lordkipanidze, D. *et al.* A fourth hominin skull from Dmanisi, Georgia. *Anat. Rec.* **288A,** 1146–1157 (2006).
8. Walker, A. & Leakey, R. *The Nariokotome* Homo erectus *Skeleton* (Springer, Berlin, 1993).
9. Brown, P. *et al.* A new small-bodied hominin from the Late Pleistocene of Flores, Indonesia. *Nature* **431,** 1055–1061 (2004).
10. Gabunia, L., Vekua, A. & Lordkipanidze, D. The environmental contexts of early human occupation of Georgia (Transcaucasia). *J. Hum. Evol.* **38,** 785–802 (2000).
11. Tappen, M., Ferring, R., Lordkipanidze, D., Vekua, A. & Kiladze, G. in *Current Topics on Taphonomy and Fossilization* (eds de Renzi, M. *et al.*) 161–170 (Ajuntament de Valencia, Valencia, 2002).
12. Vrba, E. S. A new study of the scapula of *Australopithecus africanus* from Sterkfontein. *Am. J. Phys. Anthropol.* **51,** 117–129 (1979).
13. Johanson, D. C. C. *et al.* Morphology of the Pliocene partial hominid skeleton (A.L. 288–1) from the Hadar formation, Ethiopia. *Am. J. Phys. Anthropol.* **57,** 403–451 (1982).
14. Jashashvili, T. *Hominid Upper Limb Remains from the Paleolithic Site of Dmanisi*. PhD thesis, Georgian National Museum and Univ. Ferrara (2005).
15. Weidenreich, F. Discovery of the femur and the humerus of *Sinanthropus pekinensis. Nature* **141,** 614–617 (1938).
16. Day, M. H. in *Early Hominids of Africa* (eds Jolly, C. J.) 311–345 (St Martin's Press, New York, 1978).
17. Senut, B. *L'humérus et ses articulations chez les Hominidés plio-pléistocènes* (CNRS, Paris, 1981).
18. Larson, S. G. Estimating humeral torsion on incomplete fossil anthropoid humeri. *J. Hum. Evol.* **31,** 239–257 (1996).
19. Morwood, M. J. *et al.* Further evidence for small-bodied hominins from the Late Pleistocene of Flores, Indonesia. *Nature* **437,** 1012–1017 (2005).
20. Day, M. H., Leakey R. E. F., Walker A. C. & Wood, B. A. New hominids from East Rudolf, Kenya, I. *Am. J. Phys. Anthropol.* **42,** 461–475 (1975).
21. Kennedy, G. E. A morphometric and taxonomic assessment of a hominine femur from the lower member, Koobi Fora, Lake Turkana. *Am. J. Phys. Anthropol.* **61,** 429–436 (1983).
22. Lovejoy, C. O., Meindl, R. S., Ohman, J. C., Heiple, K. G. & White, D. T. The Maka femur and its bearing on the antiquity of human walking: Applying contemporary concepts of morphogenesis to the human fossil record. *Am. J. Phys. Anthropol.* **119,** 97–133 (2002).
23. Tardieu, C. & Trinkaus, E. Early ontogeny of the human femoral bicondylar angle. *Am. J. Phys. Anthropol.* **95,** 183–195 (1994).
24. Susman, R. L. New hominid fossils from the Swartkrans formation (1979–1986 excavations): postcranial specimens. *Am. J. Phys. Anthropol.* **79,** 451–474 (1989).
25. Leakey, R. E. F. & Walker, A. C. New australopithecines from East Rudolf, Kenya (III). *Am. J. Phys. Anthropol.* **39,** 205–221 (1973).
26. Day, M. H. & Leakey, R. E. F. New evidence of the genus *Homo* from East Rudolf, Kenya (III). *Am. J. Phys. Anthropol.* **41,** 367–380 (1974).
27. Rhoads, J. G. & Trinkaus, E. Morphometrics of the Neandertal talus. *Am. J. Phys. Anthropol.* **46,** 29–43 (1977).
28. Aiello, L. & Dean, C. *An Introduction to Human Evolutionary Anatomy* (Academic, London, 1990).
29. Susman, R. L. & de Ruiter, D. J. New hominin first metatarsal (SK 1813) from Swartkrans. *J. Hum. Evol.* **47,** 171–181 (2004).
30. Susman, R. L. & Stern, J. T. Functional morphology of *Homo habilis. Science* **217,** 931–934 (1982).
31. Johanson, D. C. & Taieb, M. Plio-Pleistocene hominid discoveries in Hadar, Ethiopia. *Nature* **260,** 293–297 (1976).
32. Leakey, L. S. B., Tobias, P. V. & Napier, J. R. A new species of the genus *Homo* from Olduvai Gorge. *Curr. Anthropol.* **6,** 424–427 (1964).
33. Susman, R. L. & Creel, N. Functional and morphological affinities of the subadult hand (O.H. 7) from Olduvai Gorge. *Am. J. Phys. Anthropol.* **51,** 311–332 (1979).
34. Johanson, D. C. *et al.* New partial skeleton of *Homo habilis* from Olduavi Gorge, Tanzania. *Nature* **327,** 205–209 (1987).
35. Leakey, R. E. F., Walker, A., Ward, C. V. & Grausz, H. M. in *Hominidae* (eds Giacobini, G.) 167–173 (Jaka Books, Milan, 1989).
36. Feibel, C. S., Brown, F. H. & McDougall, I. Stratigraphic context of fossil hominids from the Omo group deposits: Northern Turkana Basin, Kenya and Ethiopia. *Am. J. Phys. Anthropol.* **78,** 595–622 (1989).
37. White, T. D. in *Encyclopedia of Human Evolution and Prehistory* (eds Delson, E., Tattersall, I., Van Couvering, J. A. & Brook, A. L.) 486–489 (Garland Publishing, New York, 2000).
38. Haeusler, M. & McHenry, H. M. Body proportions of *Homo habilis* reviewed. *J. Hum. Evol.* **46,** 433–465 (2004).
39. Richmond, B. G., Aiello, L. & Wood, B. Early hominin limb proportions. *J. Hum. Evol.* **43,** 529–548 (2002).
40. Green, D. J., Gordon, A. D. & Richmond, B. G. Limb-size proportions in *Australopithecus afarensis* and *Australopithecus africanus. J. Hum. Evol.* **52,** 187–200 (2007).
41. McHenry, H. M. Body size and proportions in early hominids. *Am. J. Phys. Anthropol.* **87,** 407–431 (1992).

42. Ruff, C. Body size prediction from juvenile skeletal remains. *Am. J. Phys. Anthropol.* **133,** 698–716 (2007).
43. Asfaw, B. *et al.* Remains of *Homo erectus* from Bouri, Middle Awash, Ethiopia. *Nature* **416,** 317–320 (2002).
44. Pontzer, H. Predicting the energy cost of terrestrial locomotion: a test of the limb model in humans and quadrupeds. *J. Exp. Biol.* **210,** 484–494 (2007).
45. Elton, S., Bishop, L. C. & Wood, B. Comparative context of Plio-Pleistocene hominin brain evolution. *J. Hum. Evol.* **41,** 1–27 (2001).
46. Rightmire, G. P. Brain size and encephalization in early to Mid-Pleistocene *Homo*. *Am. J. Phys. Anthropol.* **124,** 109–123 (2004).
47. Bramble, D. M. & Lieberman, D. E. Endurance running and the evolution of *Homo*. *Nature* **432,** 345–352 (2004).
48. Reagan, K. M. *et al.* Humeral retroversion and its relationship to glenohumeral rotation in the shoulder of college baseball players. *Am. J. Sports Med.* **30,** 354–360 (2002).
49. Stern, J. T. Jr & Susman, R. L. The locomotor anatomy of *Australopithecus afarensis*. *Am. J. Phys. Anthropol.* **60,** 279–317 (1983).
50. McHenry, H. M. How big were early hominids? *Evol. Anthropol.* **1,** 15–20 (1992).

Supplementary Information is linked to the online version of the paper at www.nature.com/nature.

Acknowledgements We acknowledge H. Herrmer for identification of cheetah remains from Dmanisi; M. Delfino for providing a revision of the amphibian and reptilian fauna; E. Trinkaus and M. Häusler for comments; G. Bumbiashvili and N. Andriashvili for the photographs; and the excavation team for constant support. Palaeomagnetic measurements were carried out at the SCT of the Barcelona University. This work was supported by a grant of the Georgian National Science Foundation, a Rolex award for enterprise, BP Georgia, the National Geographic Society, a Dan David 2003 scholarship, the Swiss National Science Foundation, the Strategic Research Funds of the University of Zurich, Wenner-Gren Foundation short-term fellowships, the Fundación Duques de Soria, a CNRS international research project grant, ECO-NET (a joint international project of the French Ministry of Foreign Affairs between France, Georgia and Azerbaijan), The Italian Ministry for Foreign Affairs (DGPCC-V), the Spanish Ministry of Education and Science, the Consejeria de Cultura de Andalucia, The National Science Foundation (USA) and the L. S. B. Leakey Foundation.

Author Contributions D.L. directs and coordinates research at Dmanisi; T.J, M.S.P.de L. and C.P.E.Z. performed comparative morphological/morphometric analyses, designed the paper and wrote the main text; G.P.R. and H.P. contributed to comparative descriptions; R.F. performed stratigraphical analyses; O.O. performed palaeomagnetic analyses; M.T. performed taphonomic analyses; G.K. organized fieldwork and prepared specimens; and A.V., M.B., J.A., R.K., B.M.-N., A.M., M.N. and L.R. performed fieldwork and provided comparative faunal analyses.

Author Information Reprints and permissions information is available at www.nature.com/reprints. The authors declare no competing financial interests. Correspondence and requests for materials should be addressed to D.L. (dlordkipanidze@museum.ge).

S1. Stratigraphy and new paleomagnetic data

Sediments in Block 2 above the 1.85 Ma Masavera Basalt are divided into two major stratigraphic units (see Fig. S1). Stratum A consists of a series of at least four separate ashfalls that conformably overlie the basalt. Stratum B deposits include horizontally extensive ashfalls, as well as a complex of deposits that filled pipes and the gullies that formed along collapsed pipes. The hominin remains in Block 2 were stratified within three subunits of Stratum B1, indicating a discrete sequence of accumulation. The first hominin bones were deposited in the lowest pipe-gully deposits of Stratum B1y, which overlies an erosional disconformity with Stratum A1. These are overlain by Stratum B1x, with numerous hominin bones that were gently scattered and quickly buried along the axis of the gully that formed along the W-E pipe axis. The superjacent gully fill (Stratum B1z), which contains one hominin remain, accumulated along a N-S axis.

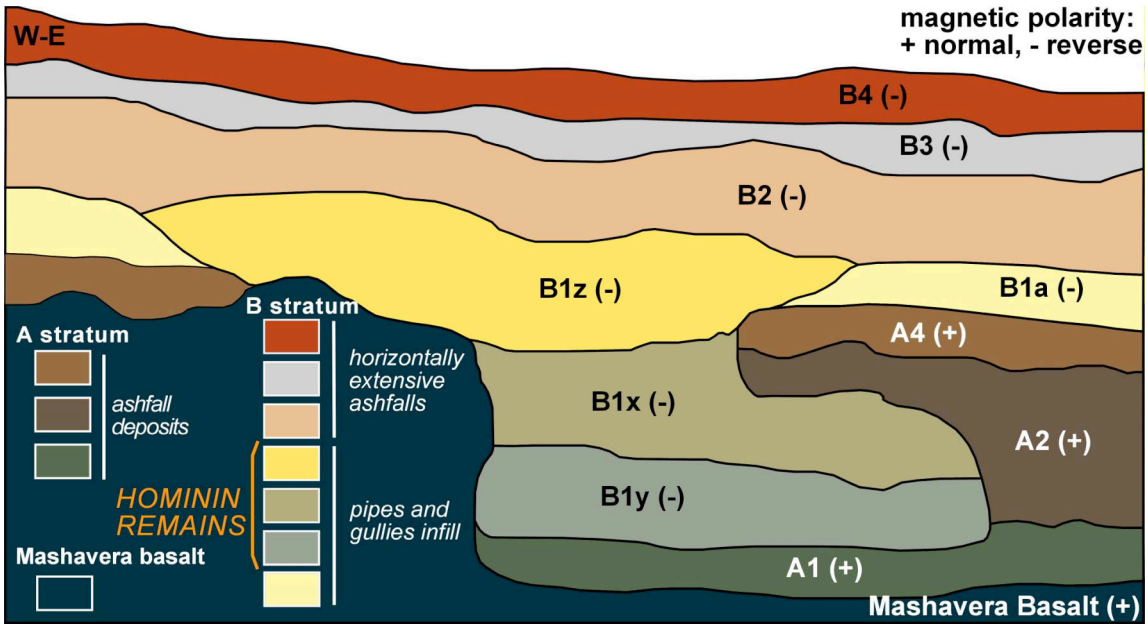

Supplementary Figure S1. Block 2 stratigraphic units, with indication of the units where hominin remains were found. Section is 10 m long, with ca. 1.8x vertical exaggeration.

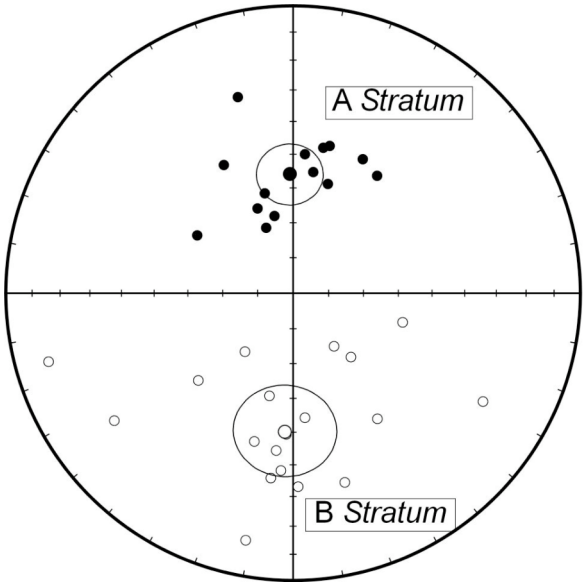

Mean directions:

	N	decl.	incl.	K	a95
Reverse (B *Stratum*)	19	183.4	-50.0	6.9	13.8
Normal (A *Stratum*)	14	358.4	55.9	20.4	9.0

Sample directions:

A samples	declination	inclination
A1B	27.5º	46.3º
A1C	346.5º	67.5º
A1D	35.6º	48.3º
A21A	9.4º	54.9º
A21B	14.0º	46.1º
A22A	11.7º	47.1º
A4C	301.1º	58.0º
A4A	4.9º	49.8º
A4B	337.2º	63.8º
ASA	17.6º	57.2º
ASB	337.7º	70.0º
ASG	331.6º	48.0º
ASH	344.2º	60.4º
ASI	344.3º	29.8º

B samples	declination	incl.
B1YB	227.3º	-53.0º
B1YBbis	219.5º	-68.5º
B1YC	146.1º	-46.2º
B1AA	190.9º	-13.5º
B1AB	234.5º	-24.6º
B1AC	254.3º	-12.6
B1ZA	104.9º	-57.6º
B1ZB	194.6º	-45.7
BY44A	174.5º	-54.1º
BY44	164.7º	-32.3º
PB2A	183.9º	-38.1º
PB2E	193.0º	-59.9º
PB2C	186.1º	-44.2º
PB2D	178.5º	-33.1º
BMA	186.9º	-35.4º
BMB	137.8º	-65.5º
BMC	182.7º	-49.3º
BME	142.5º	-71.0º
BMF	119.7º	-24.9º

Supplementary Figure S2. Individual characteristic remnant magnetization values. Left: stereographic plot (open and filled dots belong to the southern and northern hemisphere, respectively). Tables: values per sample. Note that all samples from A stratum display northern declinations and positive inclinations. Conversely, B stratum samples are southwards directed and show negative inclinations. Thus, A and B stratum display normal and reverse polarities, respectively. N=number of samples, decl. = declination, incl.= inclination, K and a95 = Fisher statistic values.

The upper part of the Stratum A deposits exhibit weak pedogenic features, and the contact between A and B is a minor erosional disconformity. The first paleomagnetic analyses of Block 2 deposits (see Figs. S1 and S2) revealed that all of the Stratum A deposits in Block 2 exhibit normal geomagnetic polarity, while all of the Stratum B1y to B2 deposits exhibit reversed polarity (adjacent to Block 2, B3 and B4 also display reversed polarity). These new data are fully concordant with the initial stratigraphic and paleomagnetic studies of Block 1[2]. Despite this change of polarity, the presence of the same rodent species of the genera *Cricetulus* and *Parameriones* in both A and B1y strata confirms that there is not a significant chronological gap between them.

S2. Fauna and biostratigraphy

Apart from the hominin record, the Dmanisi fossil vertebrate assemblage (Table S1) comprises so far remains of 44 taxa of amphibians (1), reptiles (3), birds (3) and mammals (37). Most of the micromammal species from Dmanisi correspond to typical Late Pliocene forms, such as *Mimomys pliocaenicus* and *Tcharinomys tornensis*, two characteristic voles of the Villanyian small mammal age (equivalent to the Tiglian). The large mammal association of Dmanisi reflects the time span of transition from Middle to Late Villafranchian in character. Several of the recorded elements are well known from Late Pliocene contexts in western Asia and Europe: *Pliocrocuta perrieri*, *Mammuthus meridionalis* (typical form), *Eucladoceros* aff. *tegulensis*, *Palaeotragus*, *Gallogoral meneghinii sickenbergii*. More modern forms are represented by, e.g., *Cervus* (*Pseudodama*) cf. *nestii*, *Bison* (*Eobison*) *georgicus*, and *Pontoceros* sp. The absence of raccoon dog (*Nyctereutes*) within the huge amount of recorded fossils could support the idea of a slightly younger than Middle Villafranchian mammal age.

Supplementary Table S1. Faunal list of the Dmanisi site

Class	Order	Family	Genus	Species
Amphibia				
	Anura	Bufonidae	*Bufo*	*viridis*
Reptilia				
	Testudinata	*Testudinidae*	*Testudo*	*graeca*
	Squamata	*Lacertidae*	*Lacerta*	*ex. gr. viridis*
		Colubridae	*cf. Elaphe*	*quatuorlineata*
Aves				
	Struthioniformes	Struthionidae	*Struthio*	*dmanisensis*
	Galliformes	Gallidae	*Gallus*	*dmanisiensis*
	Strigiformes	Strigidae	*Strix*	*gigas*
Mammalia				
	Insectivora	Soricidae	*Sorex*	sp.
	Lagomorpha	Ochotonidae	cf. *Ochotona*	*lagreli*
		Leporidae	cf. *Hypolagus*	*brachygnathus*
	Rodentia	Muridae	*Apodemus*	aff. *atavus*
		Cricetidae	*Cricetulus*	sp.
		Arvicolidae	*Tcharinomys*	*tornensis*
			Mimomys	*pliocaenicus*
		Gerbillidae	*Paramerione*s	aff. *obeidiensis*
		Hystricidae	*Hystrix*	*refossa*
	Carnivora	Canidae	*Canis*	*etruscus*
			Vulpes	*alopecoides*
		Ursidae	*Ursus*	*etruscus*
			Ursus	sp.
		Mustelidae	*Martes*	sp.
			Meles	sp.
		Hyaenidae	*Pliocrocuta*	*perrieri*
			Pachycrocuta	sp.
		Felidae	*Lynx*	*issiodorensis*
			Acinonyx	*pardinensis*
			Panthera	*onca* ssp.(=
			Megantereon	*megantereon*
			Homotherium	*crenatidens*
	Proboscidea	Elephantidae	*Mammuthus*	*meridionalis*
	Perissodactyla	Equidae	*Equus*	*stenonis*
			Equus	aff. *altidens*
		Rhinocerotidae	*Stephanorhinus*	*etruscus*
	Artiodactyla	Cervidae	*Cervus*	cf. *nestii*
			Cervus	*abesalomi*
			Eucladoceros	aff. *tegulensis* (= *senezensis*)
		Giraffidae	*Palaeotragus*	sp.
		Bovidae	*Bison (Eobison)*	*georgicus*
			Gallogoral	*meneghinii sickenbergii*
			Capra	*dalii*
			Soergelia	cf. *minor*
			Ovibovini indet.	
			Pontoceros	sp.
			Antilopini indet.	

S3. Palaeozoogeography

According to Fortelius *et al.*[51] the genus-level faunal resemblance index is calculated using both Simspon's[52] and Dice's[53] faunal resemblance indexes. The Dice index is the one most highly recommended by Archer and Maples[54] and Maples and Archer[55] and is calculated as 2A / (2A + B + C), where A is the number of taxa present in both faunas, B is the number of taxa present in fauna 1, but absent in fauna 2, and C is the number of taxa present in fauna 2 but absent in fauna 1. Simpson's faunal resemblance index (calculated as A / (A + E), where E is the smaller of B or C has a long tradition of use in studies of similarity of fossil mammals[56-58] and is coupled with Dice index in Figure S3**.**

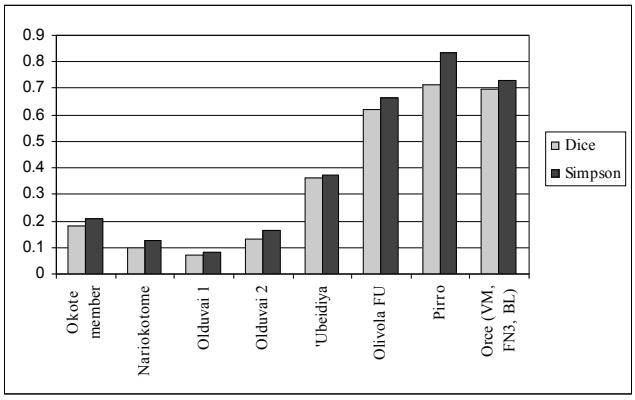

Supplementary Figure S3. Genus-level faunal comparison of Dmanisi large mammals assemblage with various Plio-Pleistocene assemblages from Africa, the Near East and Europe showing that Dmanisi has resemblance values with European Late Villafranchian mammal faunas. Data source updated by one of us (LR) from Turner *et al.*,[59] and from the Neogene of the Old World Database of Fossil Mammals (NOW public release 030717, www.helsinki.fi/science/now/).

The highest similarity values of the Dmanisi faunal assemblage are with W-European "Late Villafranchian" assemblages, while the "African" mammal faunas show very low GFRI values. Similarities between Dmanisi and African assemblages are mainly due to the co-occurrence of common carnivore genera (e.g. *Homotherium*, *Megantereon*, *Panthera*) or, among herbivores, widespread genera like *Equus*.

S4. Palaeoecology

The combination of topographic and vertebrate palaeontological information allows to infer a differentiated landscape pattern. Over a distance of a few kilometres, the landscape character changed from a flat and fairly wet river valley with gallery forests (indicated especially by the frequently recorded *Eucladoceros* and the elaphine deer *Cervus abesalomi*) to flanking slopes with shrub vegetation of varying densities, turning into dry meadows in the southerly exposed areas with more intense insolation. Extended tree savannah to open grasslands characterised the higher ground out of the valley. In addition to savannahs, semidesert-like rocky terrains existed on the lava outcrops in the vicinity of the site. *Testudo graeca* and *Hystrix refossa* indicate temperate climatic parameters.

Supplementary Table S2. Ecological characteristics of selected taxa and Dmanisi site inferred landscape

dense to open forests and shrub landscapes	tree savannah and open grasslands	rocky, semi-arid terrains
Eucladoceros aff. *tegulensis* (= *E*. aff.	cf. *Ochotona lagreli*	*Capra dalii*
		Gallogoral meneghinii
Cervus (Pseudodama) cf. *nestii*	*Parameriones* aff.	
Meles sp.		
Sorex sp.	Antilopini indet.	
Apodemus aff. *atavus*	*Equus* aff. *altidens*	
Bison (Eobison) georgicus (most probably)		
Strix gigas (most probably)		
Stephanorhinus etruscus (partly)	*Stephanorhinus etruscus*	
Mammuthus meridionalis (partly)	*Mammuthus meridionalis*	

S5. Taphonomy

The Dmanisi large mammal assemblage is well preserved with little subaerial weathering. 72% of specimens are in weathering stage 0, 21% in stage 1, and 5% in stage 2[60, 61]. This signal, along with the presence of several articulated body segments, indicates rapid burial after death. Post-burial surface damage such as fungal/root etching is common.

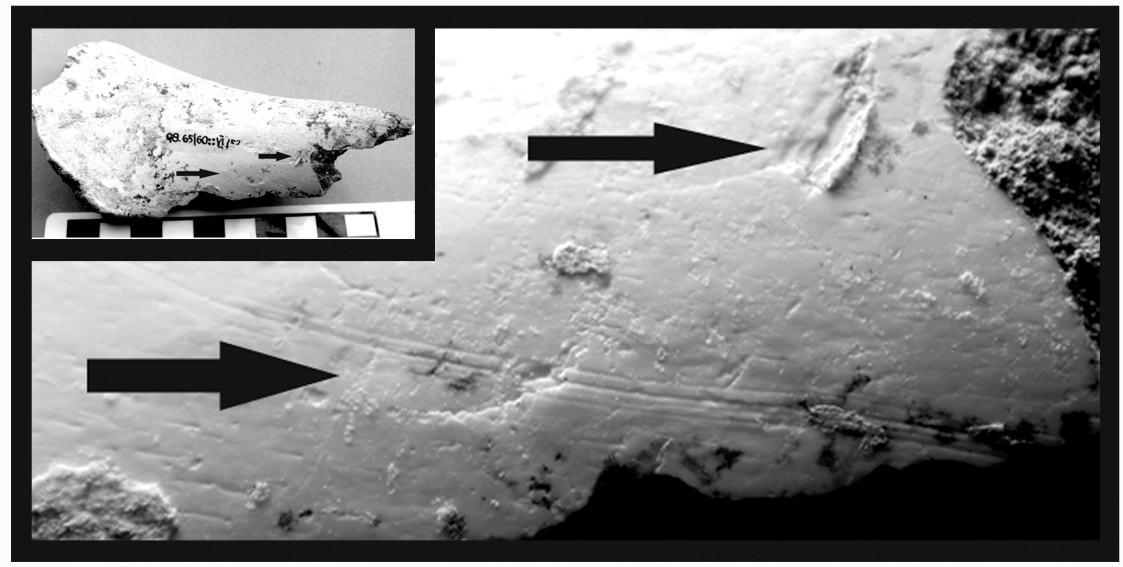

Supplementary Figure S4. Shaft fragment of a mammal size class 3 humerus with stone tool cut mark found under calcrete (lower arrow; size classes after[62]). A pit from either a hammerstone, or carnivore (upper arrow). The lack of striations in the pit suggests it is a carnivore tooth mark, which would appear to document that a carnivore broke the bone open for marrow after hominins consumed the meat. Scale bar is in cm.

One third of plotted bone specimens are unbroken. Of breaks, 50% have curved morphology and acute angles, and 21% are intermediate in form, indicating breakage while the bone was still fresh, rather than after fossilization such as breaking due to transport or crushing by sediments[63]. In addition, the absence of trample marks or other evidence of transport, suggests that most of the bones were broken during consumption.

Stone tool marks are rare, observable on less than 1% of the assemblage (see Figs. S4 and S5), but their presence does indicate that the hominins were eating meat, and with the presence of the multiple stone tools and manuports, they indicate that hominins were living in the direct vicinity of the site. The presence of cutmarks on a few mid-shaft upper limb bones (humerus/femur) indicates the hominins were filleting meat, and that a large carnivore such as a felid or hyaenid did not consume the meat first, and therefore that hominins had early access to carcasses. Carnivore tooth marks are present in higher frequencies in the assemblage than tool marks, and are on about 8-9% of the bones; hyena and other carnivore coprolites are also present. The small amount of carnivore damage is less than expected if bone-crushing hyenas accumulated the hominin bones. [64, 65]. Like the mammals, most of the hominin fossils exhibit no subaerial weathering and very little other damage. The presence of skeletal elements that almost never survive carnivore consumption, such as the 3 clavicles, first ribs, and patella, suggests that the hominins were not consumed by large carnivores[66, 67].

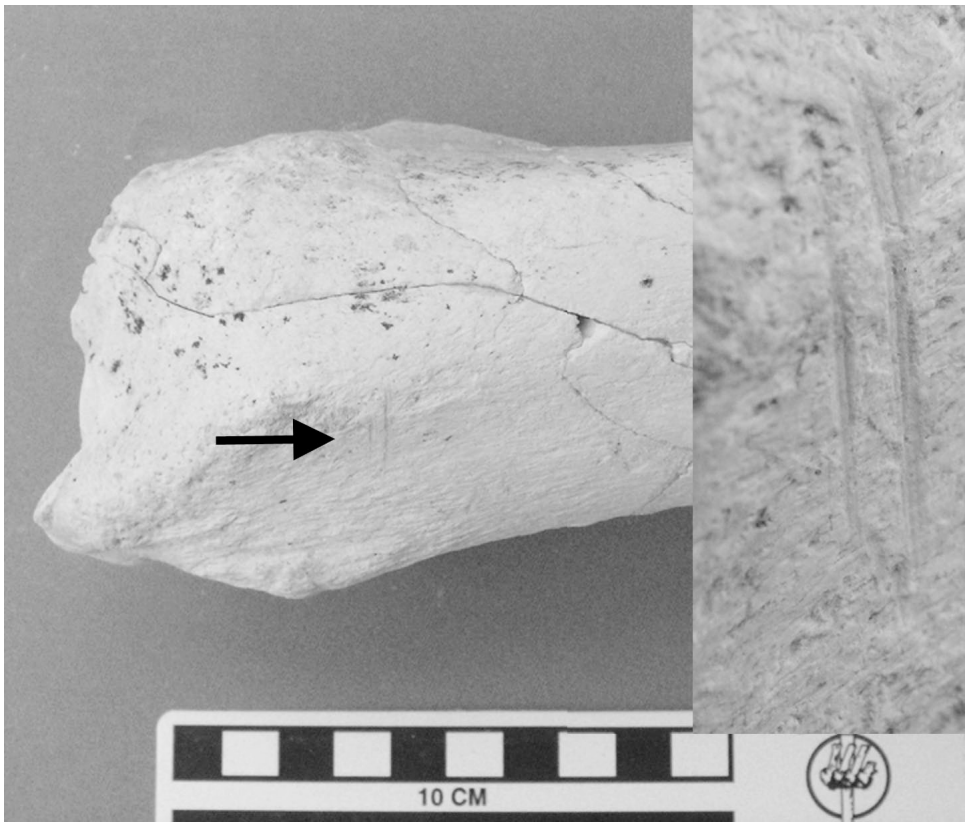

Supplementary Figure S5. *Bison* (*Eobison*) *georgicus* distal radius with a striated cut mark (1x14.9 mm) running perpendicular to the long axis.

S6. Dmanisi hominin postcranial material of subadult individual

Supplementary Table S3. Assessment of developmental stage of subadult cranial and postcranial hominin elements

Dmanisi palaeontological nr.	bone	developmental stage markers	modern human developmental age (y)[1]
D2700	cranium	third molar root 30%; spheno-occipital synchondrosis unfused	<15
D2735	mandible	agenesis of left third molar; germ of right third molar is missing	-
D2724	clavicle		-
D2715 and D2680	humerus	two out of seven secondary points of ossification are unfused: medial epicondyle and proximal epiphyses	females: 13-17 males: 14-20
D2721; D2673; D2713; D2627	vertebrae	no annular epiphyseal fusion	females: 18 males: 18.9
D2679; D2670; D3480	phalanges	epiphyseal fusion	females: 11-13 males: 14-16
D2671	metatarsal I	epiphyseal fusion incomplete	females: 13-15 males: 16-18
D2669	metatarsal IV	epiphyseal fusion	females: 11-13 males: 14-16

[1] comparative data from Scheuer & Black (ref. 68)

S7. Comparative morphometric data

Linear measurements were taken using metric callipers; maximum lengths of humerus, tibia and femur were measured using an osteometric board. Circumferences were measured with a sliding osteometric ruler. All measurements were taken to the nearest millimetre. Angular measurements were obtained from digital images using ImageJ version 1.32J (National Institutes of Health, http://isb.info.nif.gov/ij/).

The extant comparative series includes adult and subadult samples of modern *Homo sapiens*, *Pan troglodytes*, *Gorilla gorilla*, and *Pongo pygmaeus*. Samples are from the Royal Museum of Central Africa (Tervuren, Belgium), the National Museum of Natural History, Paris, and the Anthropological Institute of the University of Zurich. The modern human samples are from the archaeological sites of Karagunduz (Ankara University, Turkey) and the Necropoles of Isola Sacra, Taforalt and Afalou (Institut de Paléontologie Humaine, National Museum of Natural History, Paris).

Linear osteometric dimensions follow the definitions of Martin and Saller[69]. In the scapual, glenoid orientation relative to the spine corresponds to the angle between the base of the spine and the long axis of the glenoid cavity[70]. The glenocoracoid angle expresses the orientation of the distal extremity of the coracoid process in relation to the main axis of the glenoid cavity. In the humerus, the position of the lateral condyle is measured by the ratio between the height of the capitulum and the height of the lateral epicondyle. Because humeral heads are not preserved in the Dmanisi sample, torsion was measured on the diaphyses. Using a Microscribe 3DX digitizer, four landmarks were determined on the proximal and distal extremes of the diaphysis: on the proximal end, the most salient point in the middle of the greater tubercle (A) and the most posterior point on the anatomical neck (B); on the distal end, the most salient points on the lateral (C) and medial (D) epicondyles. Torsion was defined as the angle between vectors (A-B) and (C-D). Vertebral zygapophyseal orientation was measured, in posterior view, as the angle between the midsagittal line and a line parallel to the prezygapophyseal articular surface[71]. In C2, the anterior angle of the superior articular process was measured in anterior view between lines parallel to the left and right articular surfaces.

Supplementary Table S4. Univariate comparison of postcranial elements[1].

Measurements[2]	australopiths[3]	earliest *Homo*[3]	Dmanisi	KNM-WT15000	*Homo sapiens*[3]	*Pan troglodytes*[3]	*Gorilla gorilla*[3]
Scapula							
Olecranon direction relative to midaxillary border (M17)	116.0 – 115.0 2 [4]	-	129.0	127.0	141.7±4.7 133.8 – 154.0 30	117.7±5.8 107.7 – 128.9 30	121.8±5.3 113.3 – 132.3 29
Coracoid process width to length ratio	-	-	41.2	-	33.1±2.9 28.4 – 38.6 30	38.15±3.9 31.5 – 48.9 30	44.8±6.2 32.1 – 57.2 29
Coracoid process width			13.5		15.5±1.7 11.0 – 19.0 30	15.9±1.7 13.1 – 19.2 30	28.2±5.8 19.2 – 42.1 30
Coracoid process length			32.8		49.9±4.8 37.0 – 54.9 30	41.9±2.9 37.5 – 49.9 30	63.1±9.3 48.0 – 83.3 30
Spine process breadth to width ratio	-	-	54.0	57.7	55.2 ±5.5 42.5 – 65.4 30	16.2±4.1 10.9 – 27.9 30	16.6±3.2 10.6 – 23.0 29
Length of spine			26.3	39.53	49.3±5.9 36.9 – 59.2 30	45.8±4.9 37.2 – 54.8 30	67.3±12.2 48.2- 83.1 29
Width of spine			14.2	22.8	27.0±3.0 22.0 – 32.8 30	7.31±1.5 5.0 – 12.1 30	11.3±2.7 6.8 – 17.4 30
Glenoid orientation relative to the spine	-	-	81.0	75.0	89.4 ±6.5 79.9 – 102.9 30	55.8±7.2 41.0 – 67 30	59.0±9.6 40.0 – 78.5 29
Glenocoracoid angle			55.0	59.5	82.5±7.6 60.0 – 94.5 29	48.78±7.1 31.0 – 64.5 30	45.1±12.0 20.0 – 68.0 38
Clavicle							
Length	-	149.4[5]	137.03 – 135.6 2		137.0±10.9 113.0 - 159.0 50	118.0±11.5 97.4 – 140.2 33	148.5±15.3 126.9 – 161.2 27
			123.2	*130.5*	*127.2±7.4* *113.6 – 139.0* *13*	*106.09±8.3* *93.5 – 117.6* *8*	*148.6±15.3* *126.9- 181.2* *8*
Shape at midshaft (a-p/s-i diameters)	-	79.0[5]	79.3 – 67.2 2		76.7±9.4 57.9 – 97.3 50	70.75±10.3 46.6-89.7 33	71.0±10.4 54.9 – 100 27
			80.6	*53.8*	*80.5±11.3* *60.9 – 100* *13*	*80.2±12.1* *61.1 – 98.1* *8*	*73.4±3.6* *66.6 – 79.3* *8*
Shape at conoid tubercle (a-p/s-i diameters)	-	78.2[5]	80.6 – 80.2		60.7±11.3 40.9 – 92.3 50	42.1±4.7 33.1 – 52.6 33	52.6±5.5 38.9 – 62.6 27
			63.0	*85.1*	*62.9±9.2* *44.4 – 77.3* *13*	*39.6±4.0* *32.8 – 44.3* *8*	*52.5±4.9* *45.1 – 60.3* *8*
Humerus							
Length (M1)	235.0 – 226 2[6]	-	295.0		304.0±16.6 263.0 -341.0 38	290.3±21.6 259.0 – 326.0 33	404.8±44.7 342.0 – 466.0 31
			282.2	*319.0*	*298.2±22.7* *255.0 – 334.0* *27*	*272.7±21.0* *234.0 – 296.0* *8*	*403.6±40.3* *367.5 – 441.0* *6*
Torsion (M18)	122.7 111.0 – 130.0 4[7]	-	110.0		155.3±9.8 134.9 – 180.0 38	147.9±8.0 128.7 – 164.4 31	149.6±6.0 137.5 – 159.6 31
			104.0	*146.0*	*150.8±5.9* *138.2- 160.7* *23*	*147.7±6.1* *136.6 – 155.1* *8*	*152.6±4.7* *144.5 – 158.8* *6*
Lateral condyle position	91.5±4.7 85.0 – 98.4 7[8]	89.2[9]	85.8		112.5±11.1 92.1 – 132.3 38	76.9±6.5 62.0 – 86.9 29	73.1±4.7 63.1 – 81.6 27

Measurements[2]	australopiths[3]	earliest *Homo*[3]	Dmanisi	KNM-WT15000	*Homo sapiens*[3]	*Pan troglodytes*[3]	*Gorilla gorilla*[3]
			76.0		*109.0±15.3* *78.1 – 131.3* *21*	*103.7±14.6* *78.0 – 120.0* *8*	*66.6±6.5* *61.0 - 77.7* *6*
Vertebrae							
C2 anterior angle of sup. art. proc.	*107.0 – 120.0* *2*[10]	-	*111.0*	-	*136.0±6.4* *129.1 – 147.2* *10*	*110.5±3.2* *106.4 – 115.1* *6*	*112.3±1.4* *110.8 – 114.3* *6*
C2 canal shape (M11/M10)	-	-	*115.27*	-	*121.4±9.9* *131.9 – 108.7* *10*	*90.9 ±4.5* *85.1 – 97.7* *6*	*78.0± 6.4* *69.8 – 85.9* *6*
C3 canal shape (M11/M10)	-	-	*150.0*	-	*130.5±14.4* *113.7- 160.0* *10*	*83.1±7.3* *73.7 – 93.0* *6*	*98.3±5.0* *90.7 – 105.4* *6*
Zygapophyseal joint angles C2/C3			*62.5*		*73.4±6.8* *64.60 – 83.6* *10*	*49.6±3.6* *46.3 – 54.8* *6*	*59.6±5.9* *52.3 – 69.0* *6*
Th3 canal shape (M11/M10)	-	-	*114.8*	*110.2*	*109.5±7.8* *100.7 – 115.5* *10*	*94.4±5.5* *86.7 – 96.4* *6*	*90.8±3.5* *86.7 – 96.4* *6*
Th10 canal shape (M11/M10)	-	-	*100.8*	*100.4*	*104.2±7.6* *100.6 – 107.8* *10*	*87.9±9.4* *75.2 – 99.1* *6*	*88.4± 8.6* *76.2 – 98.6* *6*
Th10 centrum area (M4*M7)			*692.2*		*759.2±113.9* *601.1 – 958.6* *10*	*460.9±85.3* *308.0 – 565.8* *6*	*665.0±186.7* *444.6 – 964.7* *6*
Th10 centrum shape (M4/M7)			*111.6*		*136.0±13.6* *113.1 – 153.1* *10*	*121.5±9.3* *106.9 – 131.7* *6*	*126.6±10.8* *114.6 – 150.0* *6*
Th10 zygapophyseal joint angle Th10/Th11			*107.6*		*106.4±4.6* *100.0 – 113.4* *10*	*109.1±4.1* *105.3 – 115.4* *6*	*114.6±3.6* *111.0 – 119.7* *6*
L1 canal shape (M11/M10)	-	-	*80.8*	-	*87.7±8.0* *74.8 – 101.0* *10*	*115.2±6.8* *105.6 – 126.3* *6*	*120.1±11.8* *104.6 – 133.3* *6*
L1 centrum area (M4*M7)	-	-	*777.8*	*803.4*	*940.6±165.9* *706.3 – 1288.9* *10*	*772.4± 95.9* *575.4 – 836.9* *6*	*878.0± 284.8* *610.0 – 1334.0* *6*
Th10 centrum shape (M7/M4)			*114.2*		*148.8±9.0* *134.5 – 169.1* *10*	*133.5±9.2* *120.0 – 143.4* *6*	*153.7±9.7* *140.2 – 166.7* *6*
L1 zygapophyseal joint angle L1/L2	29.0[11]		*45.6*		*31.6 ±5.3* *24.5 – 40.0* *10*	*34.4±4.8* *26.8 – 38.9* *6*	*72.5±9.3* *61.6 – 84.2* *6*
Femur							
Length (M1)	280.0[12]	401.0 – 396.0 2[13]	386.0	432.0	381.9±22.9 337.0 - 434.0 22	290.2±15.9 252 - 318 30	350.1±40.8 294.0 - 423 30
Medial to lateral condylar breadth (M21c/M21e)	108.4 100.0 – 125.0[14]	87.7 – 107.9 2[13]	103.9	-	121.6±12.2 103.2 – 143.3 30	121.5±16.2 104.0 -148.6 30	139.8±14.1 119.4 – 171.8 26
Neck index (M16/M15)	69.8 64.6 – 78.2 6[15]	88.9 – 95.3 2 [13]	66.2	78.5	80.4±6.3 63.4 – 93.1 30	83.3±4.6 72.1 – 90.1 30	76.7±5.1 65.8 – 88.9 30
Bicondylar angle (M30)	77.0 75.0 – 81.0 7[16]	77.0 -80.0 2[13]	81.5	80.0	80.3±2.8 76.0 – 88.0 30	89.3±2.9 85.0-96.2 30	89.5±2.2 85.0 - 95.0 30
Tibia							
Length (M1a)	-	-	306.0	380.0	318.9±20.5 290.0 - 374.0 22	242.2±14.3 207.0 – 266.0 30	281.5±29.7 241.0 – 334.0 30
Midshaft index (M9/M8)	-	70.1 63.9 - 81.5 3[17]	66.6	83.3	60.9±6.0 48.1 – 68.2 26	67.9±6.7 56.6 – 80.5 30	76.5±7.0 62.5 – 91.4 30
Angle of torsion (M14)	-	-	21.9		20.1±7.1 7.8 – 33.8 26	33.8±6.8 21.5 – 45.8 30	27.4±5.4 20.2 – 39.3 30

Measurements[2]	australopiths[3]	earliest *Homo*[3]	Dmanisi	KNM-WT15000	*Homo sapiens*[3]	*Pan troglodytes*[3]	*Gorilla gorilla*[3]
Angle of inclination (M13)	-	-	82.0		97.2±4.6 89.1 – 111.7 26	75.1±4.5 65.4 – 82.7 30	82.5±4.4 72.3 – 90 30
Talus							
Neck angle (M16)	32.3 26.9 – 37.0 6[18]	33.5[19]	26.	-	19.4±4.9 12.0 – 31.0 30	34.4±3.9 25.4 – 42.5 30	32.4±3.8 23.5 – 36.7 30
Metatarsals							
Angle of torsion of metatarsal I (M11)	-	-	*3 – 15* *2*	-	13.9±7.1 3.5 – 32.0 30	40.1±17.4 24.2 – 54.5 28	47.5±10.8 31.4 – 68.9 30
Index of shaft of metatarsal I (M3/M4)	105.8 102.9 – 111.6 3[20]	-	*102.6 – 106.8* *2*	-	95.2±8.6 81.9 – 115.6 30	90.8±6.8 75.8 – 102.0 28	93.5±10.6 76.9 – 114.9 30
Angle of torsion of metatarsal III (M11)	-	23.6[19]	26.9 – 21.7 2	-	17.5±6.1 5.0 – 30.0 30	13.3 ±3.0 8.6 – 19.5 27	12.6±3.4 4.7 – 19.7 30
Index of shaft of metatarsal III (M3/M4)	-	63.1 – 75.3 2[21]	69-4 – 87.3 2	-	91.1±9.5 72.8 -107.0 30	74.1±6.1 64.5 - 86.6 27	74.1±8.4 53.7 – 90.9 30
Angle of torsion of metatarsal IV (M11)	-	28.2[19]	27.8 – 29.0 2	-	18.7±6.7 1.5 – 30.0 30	8.9±3.0 3.5 – 14.9 24	9.9±3.8 3.6 – 18.9 30
Index of shaft of metatarsal IV (M3/M4)	-	80.7[19]	68.1 – 75.5	-	99.6±11.4 78.3 – 122.1 30	86.5±7.2 73.9 -106.6 30	75.1±8.7 57.6 – 100.3 30
Angle of torsion of metatarsal V (M11)	-	-	6.7	-	11.7±6.4 2.8 – 27.8 30	13.2±3.8 5.8 – 23.4 30	15.9±5.6 5.9 – 26.4 30
Index of shaft of metatarsal V (M3/M4)	102.73[22]	127.80[19]	135.4	-	136.9±11.0 116.1 – 156.7 30	114.2±12.4 90.1 – 131.7 30	93.9±16.7 68.9 – 131.9 30

[1]Linear measurements are in mm, angular measurements are in degrees; [2]Measurement codes according to Martin (ref. 69); [3]Measurements are represented by mean ± std.dev., range, and sample size; data for subadults are in italics; [4]Sts7, AL288-1; [5]OH48; [6]AL288-1, Bou-VP-12/1; [7]AL288-1, ER739, Sts7, Omo119; [8]AL288-1, AL137-48, AL322-1, KP271, ER739, TM1517, Stw431c; [9]ER1504; [10]AL333-101, SK-854; [11]Sts-14f; [12]AL288-1; [13]ER1481, ER1472; [14]AL129, AL333-4, Sts34, TM1513; [15]AL288-1, AL333-3, AL333-95, F.SK26, SK82, ER1505; [16]AL288-1, AL129-1a, AL333-4, AL333w-56, Sts34, TM1513, ER993; [17]HO35a, KNM-ER813a, KNM-ER741; [18]AL288-1, TM1517, ER1476a, ER813, ER1464, Stw573; [19]OH8; [20]SK1813, SKX5017, Stw562; [21]KNM-ER1823, OH8; [22]AL333-13.

S8. Estimates of stature, body mass and encephalization quotient (EQ)

Limb proportions of the Dmanisi hominins, measured by femoro-tibial and humero-femoral ratios are similar to those of modern humans. It is thus sensible to use modern human prediction equations to estimate body mass (Table S5) and stature (Table S6) of the Dmanisi hominins.

Body mass estimates were calculated using the equations for femur, humerus, tibia, and metatarsal I[72]. The inferred body mass of the large adult individual is between 47.6 kg and 50.0 kg. The body mass of the small adult individual, calculated from the first metatarsal (D2671)[72] is 40.2 kg. Based on humeral and femoral dimensions, the body mass of the subadult is between 40.0 kg and 42.5 kg.

Stature estimates for the subadult Dmanisi individual were obtained with prediction equations for juvenile samples[42]; estimates based on humeral length (D2680) yield a value between 144.9 cm and 161.4 cm. Stature estimates for the large adult individual were obtained from humeral, femoral, and tibial dimensions[73, 74], yielding a range of 146.6 cm – 166.2 cm. Stature estimates based on the length of the first metatarsal (D3442)[75] yield a value of 143.0 cm.

Brain mass was estimated from endocranial volumes using the formula provided by Martin[76]. The encephalization quotient was evaluated according to the formula provided by Martin[77], using 95% confidence ranges for body mass estimates of each individual (Table S7).

Supplementary Table S5. Estimation of body mass in Dmanisi individuals

	specimen	Dimension1 (mm)	Dimension2 (mm)	Estimated body mass (kg)	95% confidence interval (kg)	95% confidence range (kg)	Comparative modern human sample	Data source (ref.#)
Subadult								
Elbow	D2680	38.0[1]	14.4[2]	38.5	1.3	37.2 - 39.8	female	41
		38.0[1]	14.4[2]	38.5	1.3	37.2 - 39.8	male	41
Femoral shaft	D3160	21.4[3]	25.3[4]	44.0	1.2	42.8 - 45.2	female	41
		21.4[3]	25.3[4]	44.0	1.2	42.8 - 45.2	male	41
Average				**41.2**		**40.0 - 42.5**		
Adult (large)								
Elbow	D4507	40.2[1]	17.9[2]	48.9	1.3	47.6 - 50.2	female	41
		40.2[1]	17.9[2]	48.9	1.3	47.6 - 50.2	male	41
Femoral head	D4167	40.0[5]		49.6	1.2	48.4 - 50.8	female	41
		40.0[5]		49.6	1.2	48.4 - 50.8	male	41
Proximal tibia	D3901	40.5[6]	67.3[7]	48.1	1.1	46.9 - 49.2	female	41
		40.5[6]	67.3[7]	48.1	1.1	46.9 - 49.2	male	41
Distal tibia	D3901	27.1[8]	26.0[9]	48.6	1.2	47.4 - 49.8	female	41
		27.1[8]	26.0[9]	48.6	1.2	47.4 - 49.8	male	41
Average				**48.8**		**47.6 - 50.0**		
Adult (small)								
MT I base	D3442	22.3[10]	16.4[11]	39.7			composite	72
MT I head	D3442	15.7[12]	16.3[13]	40.7			composite	72
Average				**40.2**				

[1]articular width of the distal humerus; [2]capitular height; [3,4]antero-posterior and transversal diameters of the femoral shaft, taken just inferior to the lesser trochanter; [5]maximum supero-inferior diameter of the femoral head; [6,7]antero-posterior and transversal diameter respectively of the proximal tibia; [8,9]antero-posterior and transversal diameter respectively of the talar facet on the distal tibia; [10,11]medio-lateral and dorsoplantar diameter respectively of the base of metatarsal I; [12,13]medio-lateral and dorsoplantar diameter respectively of the head of metatarsal.

Supplementary Table S6. Estimation of stature in Dmanisi individuals

		Length (cm)	Stature estimate (cm)	95% confidence interval (cm)	95% confidence range (cm)	Comparative sample	data source (ref. #)
Subadult							
Humerus	D2680	28.2	152.7	8.6	144.1 - 161.4	subadult (12y)	42
		28.2	153.5	7.9	145.6 - 161.5	subadult (13y)	42
Average			**153.1**		**144.9 - 161.4**		
Adult (large)							
Humerus	D4507	29.5	161.5	11.1	150.4 - 172.5	Caucasian (m)	73
		29.5	159.6	9.6	149.9 - 169.2	Caucasian (f)	73
		29.5	159.6	10.4	149.2 - 169.9	African (m)	73
		29.5	158.0	9.2	148.8 - 167.3	African (f)	73
		29.5	145.7			African (m)	78
		29.5	143.0			African (f)	78
Femur	D4167	38.6	154.5	9.2	145.3 - 163.7	Caucasian (m)	73
		38.6	152.6	8.6	144.1 - 161.2	Caucasian (f)	73
		38.6	155.7	11.2	144.4 - 166.9	African (m)	73
		38.6	151.2	8.3	142.8 - 159.5	African (f)	73
		38.6	138.5			African (m)	78
		38.6	134.3			African (f)	78
Tibia	D3901	30.0	157.2	10.0	147.2 - 167.3	Caucasian (m)	73
		30.0	153.6	10.3	143.3 - 163.9	African (m)	73
		30.0	133.6			African (m)	78
		30.0	130.5			African (f)	78
Average			**149.3**		**146.6 - 166.2**		
Adult (small)							
Mt I	D3442	4.74	**143.0**			Combined data	75

Supplementary Table S7. Estimation of encephalization quotient (EQ)

Individual	Estimated brain mass (g)	Estimated average body mass (kg)	EQ
subadult	560	41.2	2.96
		49.4[1]	2.57
large adult	632[2]	48.8	2.94
small adult	582	40.2	3.13

[1] estimated body mass at adulthood (120% of 41.2 kg)
[2] average of D2280, D2700, and D3444

S9. Character states identified in the Dmanisi postcranial remains

Table S8 summarizes states for characters identified on the Dmanisi postcranial remains and provides a tentative ordering of character states from primitive (dark shading) versus derived (light shading or white). The Dmanisi hominins exhibit an array of symplesiomorphic characters that group them with australopiths and earliest *Homo*, while KNM-WT15000 appears more derived in several features. KNM-WT15000 and Dmanisi share an array of synapomorphies with modern humans but are more primitive than modern humans in most features.

Supplementary Table S8. Character states of Dmanisi postcranial elements

	chimpanzees	australopiths	earliest *Homo*	Dmanisi	*H. erectus* (WT15000)	modern humans
Scapula						
orientation of glenoid cavity	cranial	cranial	-	cranial	cranial	lateral
l/w ratio of coracoid process	high	-	-	high	-	low
glenocoracoid angle	narrow	-	-	narrow	narrow	wide
b/l ratio of spine	low	-	-	high	high	high
Clavicle						
shaft length relative to humeral length	long	-	-	middle	middle	short
shape of conoid tubercle (relative a-p diameter)	small	-	large	large	large	large
Humerus						
position of lateral epicondyle rel. to lat. condyle	high	middle	middle	middle	-	low
degree of torsion	high	low	-	low	middle	high
Vertebrae						
canal shape (direction of greatest width)	dorsoventral	transversal	-	transversal	transversal	transversal
C2 spinal process	long	short	-	short	-	short
C2 sup. articular surface angle	narrow	narrow	-	narrow	-	wide
Th&L centrum area relative to body mass	small	middle	-	middle	middle	large
thoracic zygapophyseal joint angle	wide	middle	-	middle	wide	narrow
lumbar zygapophyseal joint angle	narrow	narrow	-	slightly wide	narrow	narrow
wedging of lumbar vertebrae	anterior	posterior	-	posterior	posterior	posterior
Femur						
elevation of greater trochanter	high	middle	middle	middle	-	low
bicondylar angle	wide	narrow	narrow	narrow	narrow	narrow
Tibia						
rel. size of joint surfaces	large	-	-	large	-	small
degree of torsion	high	-	-	low	-	low
Talus						
neck angle	wide	middle	middle	middle		narrow
flexor hallucis longus groove	deep, longitudinal	-	-	shallow, oblique	-	shallow, vertical
medial tubercles	2 prominent tubercles	-	-	2 prominent tubercles	-	prominent lateral tubercle
Metatarsals						
Mt1 torsion	wide	-	-	narrow	-	narrow
Mt I head size	small	large	large	large	-	large
Mt III, IV shaft torsion	narrow	-	wide	wide	-	wide
transversal and longitudinal pedal arching	absent	-	present	present	-	present
Body dimensions						
limb proportions (humerus/femur ratio)	high	middle	low	low	low	low
body mass	low	low	middle	middle	high	high
EQ	2.38	2.4 – 3.1	3.1	2.7 – 2.8	2.7 – 3.8	6.28

Supplementary References (continued from main text)

51. Fortelius, M., Werdelin, L., Andrews, P., Bernor, R. L., Gentry, A. *et al.* in *The Evolution of Western Eurasian Neogene Mammal Faunas* (eds. Bernor, R. L., Fahlbusch, V. & Mittmann, H.-W.) 414-448 (Columbia University Press, New York, 1996).
52. Simpson, C. G. Mammals and the nature of continents. *Am. J. Sci.* **241**, 1-31 (1943).
53. Sokal, R. R. & Sneath, P. H. A. *Principles of Numerical Taxonomy* (Freeman and Co, San Francisco, 1963).
54. Archer, A. W. & Maples, C. G. Monte Carlo simulation of selected binomial similarity coefficients: effect of number of variables. *Palaios* **2**, 609-617 (1987).
55. Maples, C. G. & Archer, A. W. Monte Carlo simulation of selected binomial similarity coefficients (2): effect of sparse data. *Palaios* **3**, 95-103 (1988).
56. Bernor, R. L. in *New Interpretations of Ape and Human Ancestry* (eds. Ciochon, R. L. & Corruccini, R.) 21-64 (Plenum Press, New York, 1983).
57. Flynn, L. Faunal provinces and the Simpson coefficient. *Contrib.Geology, Univ. Wyoming Spec.* **3**, 317-338 (1986).
58. Bernor, R. L. & Rook, L. in *Recent Advances on Multidisciplinary Research at Rudabánya, Late Miocene (MN9), Hungary: a Compendium* (eds. Bernor, R. L., Kordos, L. & Rook, L.) 21-25 (Palaeontographia Italica, Pisa, 2003).
59. Turner, A. e. a. in *African Biogeography, Climate Change and Human Evolution* (eds. Bromage, T. G. & Schrenk, F.) 369-399 (Oxford University Press, 1999).
60. Tappen, M., Lordkipanidze, D., Bukshianidze, M., Vekua, A. & Ferring, R. in *African Taphonomy: A Tribute to the Career of C.K. "Bob" Brain* (eds. Pickering, T. R., Schick, K. & Toth, N.) (Oxford University Press, Bloomington, Indiana,, 2006).
61. Behrensmeyer, A. K. Taphonomic and ecologic information from bone weathering. *Paleobiology* **2**, 150-162 (1978).
62. Brain, C. K. *The Hunters or the Hunted* (University of Chicago Press, Chicago, 1981).
63. Villa, P. & Mahieu, E. Breakage patterns of human long bones. *J. Hum. Evol.* **21**, 27-48 (1991).
64. Horwitz, L. & Smith, P. in *Proceedings of the 1993 Bone Modification Conference* (eds. Hannus, L., Rossum, L. & Winham, R.) 188-194 (Archeology Laboratory, Augustana College, Hot Springs, South Dakota, 1993).
65. Horwitz, L. K. & Smith, P. The effects of striped hyaena activity on human remains. *J. Archaeol. Sci.* **15**, 471 - 481 (1988).
66. Haglund, W. D. & Sorg, M. H. *Forensic Taphonomy: the Postmortem Fate of Human Remains* (CRC Press LLC, Boca Raton, 1996).
67. Pickering, T. Carnivore voiding: A taphonomic process with the potential for the deposition of forensic evidence. *J. Archaeol. Sci.* **46**, 401-411 (2001).
68. Scheuer, L., Black, S. & Christie, A. *Developmental Juvenile Osteology* (Academic Press, California, 2000).
69. Martin, R. *Lehrbuch der Anthropologie in systematischer Darstellung mit besonderer Berücksichtigung der anthropologischen Methoden* (Fischer, Stuttgart, 1957-1966).

70. Etter, H. F. L'omoplate des primates supérieurs, la relation entre sa forme et sa function. *Archives Suisses d'Anthropologie Générale (Genève)* **48**, 31-51 (1984).
71. Singer, K. P., Breidahl, P. D. & Day, R. E. Variations in zygapophyseal joint orientation and level of transition at the throracolumbar junction. *Surg. Radiol. Anat.* **10**, 291-295 (1988).
72. McHenry, H. M. & Berger, L. R. Body proportions of *Australopithecus afarensis* and *A. africanus* and the origin of the genus *Homo*. *J. Hum. Evol.* **35**, 1-22 (1998).
73. Trotter, M. & Gleser, G. C. Estimation of stature from long bones of American Whites and Negroes. *Am J Phys Anthropol* **10**, 463–514 (1952).
74. Duyar, I. & Pelin, C. Body height estimation based on tibia length in different stature groups. *Am. J. Phys. Anthropol.* **122**, 23-27 (2003).
75. Byers, S., Akoshima, K. & Curran, B. Determination of adult stature from metatarsal length. *Am. J. Phys. Anthropol.* **79**, 275-279 (1989).
76. Martin, R.D. Adaptation and body size in primates. *Z. Morphol. Anthropol.* **71**, 115-124 (1980).
77. Martin, R. D. Relative brain size and basal metabolic rate in terresrial vertebrates. *Nature* **293**, 57-60 (1981).
78. Lundy, J. K. & Feldesman, M. R. Revised equation for estimating living stature from the long bone of the South African Negro. *S. Afr. J. Sci.* **83**, 54-55 (1987).